References

BERGHUIS, J., HAANAPPEL, IJ. M., POTTERS, M., LOOPSTRA, B. O., MACGILLAVRY, C. H. & VEENENDAAL, A. L. (1955). *Acta Cryst.* **8**, 478.

BONAMICO, M., DESSY, G., MARIANI, C., VACIAGO, A. & ZAMBONELLI, L. (1965). *Acta Cryst.* **19**, 619.

BONAMICO, M., DESSY, G., MUGNOLI, A., VACIAGO, A. & ZAMBONELLI, L. (1965). *Acta Cryst.* **19**, 886.

BONAMICO, M., MAZZONE, G., VACIAGO, A. & ZAMBONELLI, L. (1965). *Acta Cryst.* **19**, 898.

DAUBEN, C. H. & TEMPLETON, D. H. (1955). *Acta Cryst.* **8**, 841.

DUNITZ, J. D. (1957). *Acta Cryst.* **10**, 307.

GILLESPIE, R. J. (1963). *J. Chem. Soc.* pp. 4672, 4679.

HARDING, M. M. & COLE, S. J. (1963). *Acta Cryst.* **16**, 643.

HIGGINS, G. M. C. & SAVILLE, B. (1963). *J. Chem. Soc.* p. 2812.

International Tables for X-ray Crystallography (1959). Vol. II, p. 295. Birmingham: Kynoch Press.

KLUG, H. P. (1966). *Acta Cryst.* **21**, 536.

PAULING, L. (1960). *The Nature of the Chemical Bond.* 3rd ed. p. 246. Ithaca: Cornell Univ. Press.

Tables of Interatomic Distances and Configuration in Molecules and Ions (1958). Special Publication No. 11. London: The Chemical Society.

THOMAS, L. H. & UMEDA, K. (1957). *J. Chem. Phys.* **26**, 239.

VACIAGO, A. (1960). *Rend. Accad. Lincei* VIII, **28**, 851.

Acta Cryst. (1967). **22**, 81

An X-ray Study of the Effect of Manganese on the Occurrence of Stacking Faults in Silver-Base Alloys

BY S. P. SEN GUPTA AND K. N. GOSWAMI

Indian Association for the Cultivation of Science, Calcutta 32, *India*

(*Received* 5 *April* 1966)

X-ray diffraction line profiles from filings of silver–manganese alloys in the solid-solution range were recorded by a Geiger counter X-ray diffractometer. Stacking-fault parameters α and β were obtained from peak position and peak asymmetry measurements and the concentration of deformation faults has been found to be negligibly small. The broadening of the powder-pattern peaks was studied by Fourier analysis of line shapes and the anisotropic values of the effective particle sizes $[D_e]_{hkl}$ and the root-mean-square strains $[\langle\varepsilon_L^2\rangle]_{hkl}^{1/2}$ were obtained in all cases. Appreciable change in $[D_e]_{hkl}$ was not observed across the solid-solution range and the measured effective particle sizes are primarily a consequence of deformation and twin faulting. A good agreement was observed for the compound fault probability $(1{\cdot}5\alpha+\beta)$ obtained by two different methods.

Introduction

During recent years a great deal of attention has been given to the X-ray diffraction study of cold-worked metals and alloys as it is able to reveal a fairly detailed picture of the deformed state. It has been observed that cold working produces appreciable changes in the intensity distribution of diffracted X-rays and it is well established that the broadening of X-ray powder diffraction line profiles of f.c.c. metals and alloys results from a reduction in the size of the coherently diffracting domains, from distortion within these coherent domains and from stacking faults on (111) planes. Besides peak broadening, peak shift and peak asymmetry are also observed and are chiefly due to deformation and twin stacking faults (Warren, 1959).

Since stacking faults exert an important influence on the structural and mechanical properties of f.c.c. metals and alloys, extensive measurements on the occurrence of stacking faults in binary alloys based on the solvent metals copper and silver have been performed (Warren & Warekois, 1955; Wagner, 1957; Davies & Cahn 1962; Adler & Wagner, 1962; Foley, Cahn & Raynor, 1963; Vassamillet & Massalski, 1964; Sen Gupta & Quader, 1966; Goswami, Sen Gupta & Quader, 1966*a*). All these investigations have shown pronounced increase of the faulting probability with increasing solute content and the dependence of stacking fault parameter α on solute concentration is either linear or roughly parabolic. Recently, to observe the effects of the transition metals manganese and nickel on the occurrence of stacking faults in copper-base alloys, measurements have been carried out by Henderson (1963–64), Nakajima & Numakura (1965) and Goswami, Sen Gupta & Quader (1966*b*) and a quite different and interesting picture has been obtained in these systems. The concentration of stacking faults has been found to be small and the variation of the fault parameter α with increasing solute content is neither linear nor parabolic.

In view of this, the present investigation, which is concerned with the observation of the effect of transition solute manganese on the occurrence of stacking faults in silver-base alloys, has been taken into consideration and Warren & Averbach's method (Warren, 1959) of Fourier analysis of line shapes has been

employed for the evaluation of particle size, compound fault probability and micro-strain in the cold-worked state.

Experimental procedure

Silver-manganese alloys in the solid solution range were prepared from spectrographically standardized silver and manganese supplied by Messrs Johnson, Matthey & Co. Ltd, London. Accurately weighed quantities of the component metals were melted together in evacuated and sealed quartz capsules; after melting, the alloys were homogenized for a week at 800 °C. The annealing treatments were terminated by quenching in air. Weight changes during preparation were negligible.

Cold-working was carried out by hand filing at room temperature (28 ± 1 °C). A sample of the filings was retained in the 'as-filed' condition and another sample was annealed at 600 °C for 4 hours in a Pyrex glass capsule sealed under vacuum. The filings were sieved through a 250-mesh screen and filled into the sample holder, a solution of Canada balsam in xylene being used as a binder. The line profiles were recorded at room temperature (28 ± 1 °C) with a standard Philips Geiger Counter X-ray Diffractometer (PW 1050, 1051) using nickel filtered Cu $K\alpha$ radiation from a highly stabilized X-ray generator (PW 1010). The line shapes were recorded manually and measurements were made of the diffracted intensity at intervals in 2θ varying from 0·1° in the general background to 0·01° near the maxima of the peaks, where θ is the Bragg angle. The systematic reflexions 111, 200, 222 and 400 were studied in detail.

Stacking fault measurements

The deformation fault probability α has been obtained from measuring the change in position of 111, and 200 reflexions, using the relation (Wagner, 1957):

$$(2\theta^{\circ}_{hkl}-2\theta^{\circ}_{h'k'l'})_{CW}-(2\theta^{\circ}_{hkl}-2\theta^{\circ}_{h'k'l'})_{Ann}=H.\alpha \qquad (1)$$

and $$H=(\langle G\rangle j\,.\,\tan\theta^{\circ})_{hkl}-(\langle G\rangle j\,.\,\tan\theta^{\circ})_{h'k'l'}$$

where j is the fraction of (hkl) planes affected by deformation faults, $G=(\pm)90\sqrt{3}\,.\,h_3/\pi^2 l_0^2$ and $\langle G\rangle$ is the averaged value for the hkl reflexions affected by deformation faults.

The peak positions of 111 and 200 reflexions were determined by the same method as adopted earlier (Sen Gupta & Quader, 1966), *i.e.* by taking the mid-points of section lines drawn parallel to the background level and extrapolating to the peak maximum. The estimated accuracy of the position measurements was about ±0·01° in 2θ. Elimination of the α_2 component in the case of cold-worked peaks was not possible since the graphical methods of Rachinger (1948) and of Papoulis (1955) could not be applied for broad, overlapping and asymmetric line profiles. Owing to statistical fluctuations, points of maximum intensity cannot be also taken as a position for the peak maximum.

Twin faults have been found to broaden the diffraction-line profiles asymmetrically. The asymmetry may also be produced by segregation of the solutes to the stacking faults, according to the theory of Willis (1959). However, it is difficult to detect (Suzuki, 1962) and also to eliminate from that due to twin faults. Cohen & Wagner (1962) have developed a method of determining twin-fault probability β by measuring the displacement of the centre of gravity of a peak from the peak maximum. The following relation is involved in the determination of β from 111 and 200 peaks:

$$\beta=\frac{\Delta\text{C.G.}\,(^{\circ}2\theta)_{111}-\Delta\text{.C.G}\,(^{\circ}2\theta)_{200}}{11\tan\theta_{111}+14{\cdot}6\tan\theta_{200}}. \qquad (2)$$

The method of Ladell, Parrish & Taylor (1959) has been adopted for the determination of the centre of gravity (C.G.) of line profiles. Prior to actually evaluating C.G., each peak height was divided by the factor (Warren, 1959) $f^2(1+\cos^2 2\theta)/\sin^2\theta$ where f is the atomic scattering factor. Experimental limitations (such as long tails of the peak, peak overlap and error in peak maximum position determination) do not enable us to determine ΔC.G. accurately and hence β with sufficient accuracy.

Values of α and β for Ag–Mn alloys are inserted in Table 1 and the variation of α with solute content for Ag–Mn and Cu–Mn alloys (Goswami *et al.* 1966*b*) is shown in Fig. 1.

Peak broadening measurements

Warren & Averbach's method (Warren, 1959) of Fourier analysis of line shapes provides information concerning the effective particle size, the root mean square strain and the compound fault probability $(1{\cdot}5\alpha+\beta)$. The 111, 222, 200 and 400 reflexions were

Table 1. *Experimental results for silver–manganese alloys*

Composition (at. %)	$\alpha\times10^3$	$\beta\times10^3$	$(1{\cdot}5\alpha+\beta)_{P+A}\times10^3$	$(1{\cdot}5\alpha+\beta)_B\times10^3$
Ag– 5·54 Mn	3·27	11·89	17	21
Ag–11·03 Mn	3·71	14·04	20	19
Ag–16·20 Mn	3·93	13·03	19	17
Ag–20·92 Mn	3·27	11·17	16	17

Composition (at. %)	$[D_{SF}]_{111}$ (Å)	$[D_e]_{111}$ (Å)	$[D_e]_{100}$ (Å)	T_{min} (Å)	$[\langle\varepsilon_L{}^2{}_{=50\text{Å}}\rangle]_{111}{}^{\ddagger}\times10^3$	$[\langle\varepsilon_L{}^2{}_{=50\text{Å}}\rangle]_{100}{}^{\ddagger}\times10^3$
Ag– 5·54 Mn	562	235	139	311	2·28	4·41
Ag–11·03 Mn	491	209	134	228	2·50	4·47
Ag–16·20 Mn	509	188	131	176	2·53	4·08
Ag–20·92 Mn	586	185	128	175	2·74	3·60

chosen, as with these it is possible to determine particle sizes and lattice strains in the [111] and [100] directions. Initially, Stokes's (1948) method has been applied for the correction of instrumental broadening and it has been assumed that line shapes obtained from the samples annealed for 4 hours at 600°C are, in each case, an exact measure of instrumental broadening. Beevers–Lipson strips were employed for the evaluation of Fourier coefficients expressing the line shapes and the corrected coefficients were represented as A_L *versus* L where L $(=na_3)$ has the significance of a distance normal to the reflecting planes.

The measured coefficients A_L may be written as:

$$\ln A_L(h_0)=\ln A_L^P+\ln A_L^D(h_0) \qquad (3)$$

where A_L^P are the particle size coefficients and A_L^D are the distortion coefficients dependent upon $h_0=(h^2+k^2+l^2)^{\frac{1}{2}}$, the order of reflection.

The intercept of the initial slope of the order independent Fourier coefficient A_L^P with the abscissa L gives the effective particle size $[D_e]_{hkl}$. Normal corrections (Warren, 1959) were applied for the observed 'Hook effect'. As shown by Warren (1961), the effective particle size may be written in terms of the coherently diffracting domain size D normal to the reflecting planes, the deformation and twin fault probability α and β, the domain size T in the faulting plane and the lattice parameter a:

$$\frac{1}{[D_e]_{111}}=\frac{1}{D}+\frac{1}{\sqrt{2}T}+\frac{\sqrt{3}}{4a}(1{\cdot}5\alpha+\beta) \qquad (4)$$

$$\frac{1}{[D_e]_{100}}=\frac{1}{D}+\frac{1}{\sqrt{1{\cdot}5}T}+\frac{1}{a}(1{\cdot}5\alpha+\beta). \qquad (5)$$

The inverse of the last term is referred to as D_{SF}, the fictitious domain size due to faulting. A minimum value of T, $T_{\min}$, is given by (Warren, 1961):

$$T_{\min}=\frac{0{\cdot}82}{\left[\frac{2{\cdot}31}{[D_e]_{111}}-\frac{1}{[D_e]_{100}}\right]}. \qquad (6)$$

The r.m.s. strain component as a function of distance L has been measured for [111] and [100] directions, using the strain dependent Fourier coefficients.

Table 1 summarizes the values of $[D_e]_{hkl}$, D_{SF}, $T_{\min}$ and $[\langle\varepsilon^2_{L=50\text{Å}}\rangle]^{1/2}_{hkl}$ (r.m.s. strain at an average distance $L=50$ Å) for Ag–Mn alloys. Figs. 2 and 3 show the plots of A_L^P and $\langle\varepsilon_L^2\rangle^{\frac{1}{2}}$ as a function of distance L for [111] and [100] directions in Ag–20·92%Mn and Ag–11·03%Mn alloys respectively.

Discussion

It is apparent from Table 1 and also from Fig. 1 that the concentration of deformation stacking faults in silver–manganese alloys across the primary solid solution range is negligibly small compared with that of other elements alloyed with silver (Davies & Cahn, 1962; Adler & Wagner, 1962; Sen Gupta & Quader, 1966) and the values are also less than those obtained for copper–manganese alloys. It may be mentioned here that the value of α for pure silver is also less than that for pure copper. As seen from Fig. 1, in copper–manganese alloys the values of α increase slowly from $3{\cdot}77\times10^{-3}$ (for pure Cu) to $8{\cdot}72\times10^{-3}$ (for Cu–22·34% Mn) reaching a saturation at about 14 at.% manganese solute. Thus, it may be inferred that the contribution of the transition element manganese in silver and copper alloys to the stacking fault parameter is very small and is probably due to the interactions between the incomplete $3d$ shells of the introduced solute atoms which provide an additional contribution to the stacking fault energy of the alloy (Seeger, 1955, 1957).

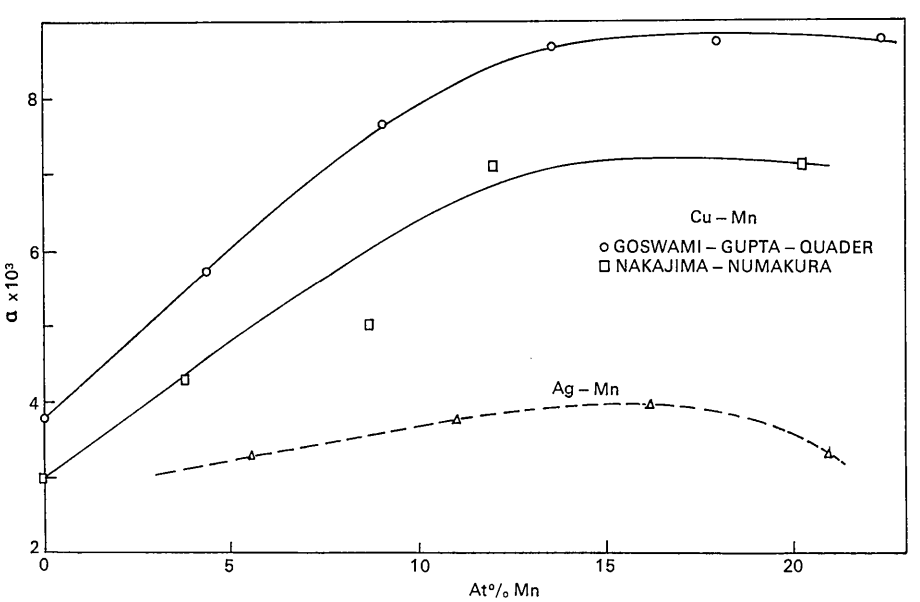

Fig. 1. Deformation fault probability α as a function of manganese concentration in silver and copper alloys.

In fact, Imura, Suzuki, Ikushima & Marukawa (1963), in their measurements of stacking fault energy for copper alloys containing upto 10·2 at.% manganese by transmission electron microscopy, were unable to observe any appreciable effect.

In comparison with deformation faults, the concentration of twin faults appears to be more and does not change appreciably with increasing manganese content. However, not much reliance can be placed on the values of β as the method suffers from experimental limitations.

The anisotropy of effective particle sizes and lattice strains has been clearly observed, as is evident from Table 1 and Figs. 2 and 3. As is apparent from Table 1, appreciable decrease in the effective particle size values is not observed here, whereas in copper–manganese alloys (Goswami *et al.*, 1966*b*) a steady decrease of particle size values from 344 to 155 Å and 252 to 98 Å for [111] and [100] directions respectively has been observed reaching saturation at about 18 at.% manganese solute. This may be explained when the role of stacking faults in the observed particle size broadening is taken into consideration. In the present case, the average experimental ratio of $[D_e]_{111}/[D_e]_{100}$ is about 1·5 and this indicates that D and more likely T (as $T_{\min}$ is of the order of $[D_e]_{111}$) also influence the magnitudes of the measured effective particle sizes. This is further supported by the computed values of $[D_{SF}]_{111}$. In copper–manganese alloys (Goswami *et al.*, 1966*b*) the concentration of stacking faults is slightly more and the role of stacking faults in the particle size broadening is significant.

Measured anisotropic particle sizes also yield the compound fault probability $(1{\cdot}5\alpha+\beta)$ (Adler & Wagner, 1962) and it has been observed (Table 1) that the values of $(1{\cdot}5\alpha+\beta)$ obtained from particle size measurements $\left(\text{with the assumption that } \frac{1}{D}+\frac{1}{\sqrt{2}T}=\frac{1}{D}+\frac{1}{\sqrt{1{\cdot}5}T}\right)$ are in good agreement with the values obtained from peak position and peak asymmetry measurements.

For all the specimens the r.m.s. strains have been found to decrease asymptotically with increasing distance L from the reflecting plane (Fig. 3), and the same form of the curve was also observed in copper–manganese alloys (Goswami *et al.*, 1966*b*) and in the study of other f.c.c. alloys (Warren & Warekois, 1955; Adler & Wagner, 1962; Sen Gupta & Quader, 1966; Goswami *et al.*, 1966*a*). The ratio of r.m.s. strains measured at $L=50$ Å is about 1·7 and this observed anisotropy of strain cannot be accounted for by the simple isotropic stress model according to which the residual microstrains in the $[hkl]$ directions will be inversely proportional to the directional Young's modulus. For pure silver (Huntington, 1958), the ratio $E_{111}/E_{100}=2{\cdot}7$, and thus the observed anisotropy is probably related to the non-uniform distribution of dislocations and to the stress directionality of dislocations and stacking faults. In copper–manganese alloys (Goswami *et al.*, 1966*b*), the ratio of r.m.s. strains was found to be 1·5 and the same inference has been drawn.

The authors are grateful to Prof. B. N. Srivastava, D.Sc., F.N.I., for his continued interest in the work and

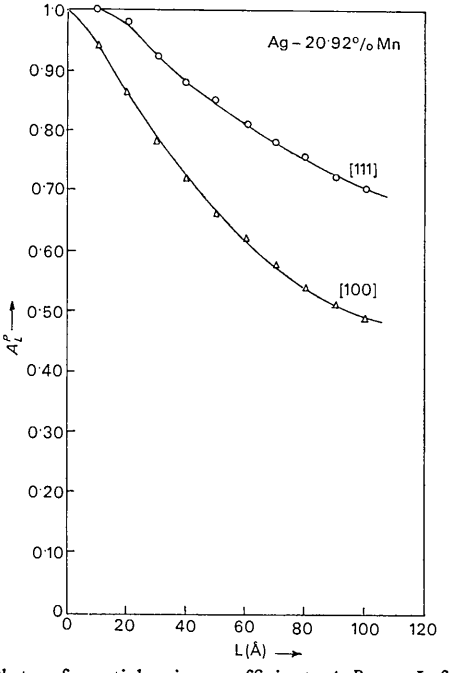

Fig. 2. Plots of particle size coefficient $A_L{}^P$ *vs.* L for [100] and [111] directions for cold-worked Ag–20·92 %Mn alloy.

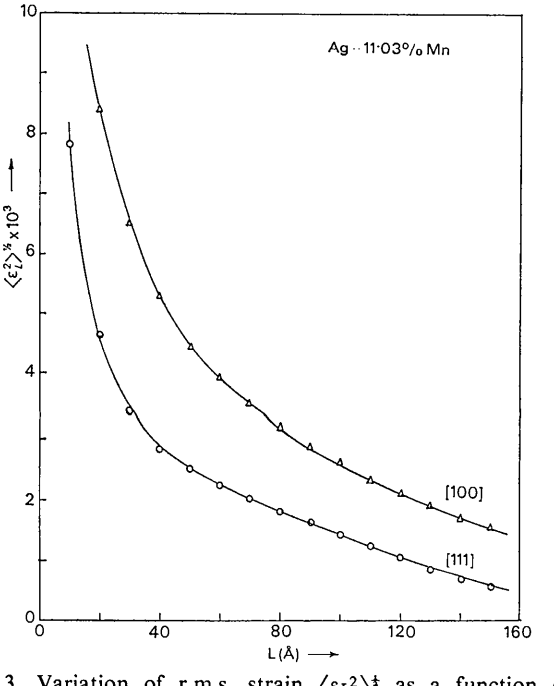

Fig. 3. Variation of r.m.s. strain $\langle \varepsilon_L{}^2 \rangle^{\frac{1}{2}}$ as a function of averaging distance L for [100] and [111] directions for cold-worked Ag–11·03 %Mn alloy.

to Dr M.A.Quader for helpful discussions. One of the authors (S.P.S.G.) is thankful to the C.S.I.R. (New Delhi) for financial assistance.

References

ADLER, R. P. I. & WAGNER, C. N. J. (1962). *J. Appl. Phys.* **33**, 3451.
COHEN, J. B. & WAGNER, C. N. J. (1962). *J. Appl. Phys.* **33**, 2073.
DAVIES, R. G. & CAHN, R. W. (1962). *Acta Metallurg.* **10**, 621.
FOLEY, J. H., CAHN, R. W. & RAYNOR, G. V. (1963). *Acta Metallurg.* **11**, 355.
GOSWAMI, K. N., SEN GUPTA, S. P. & QUADER, M. A. (1966*a*). *Acta Cryst.* **21**, 243.
GOSWAMI, K. N., SEN GUPTA, S. P. & QUADER, M. A. (1966*b*). *Acta Metallurg.* In the press.
HENDERSON, B. (1963–64). *J. Inst. Metals*, **92**, 55.
HUNTINGTON, H. B. (1958). *Solid State Physics*, **7**, 213.
IMURA, T., SUZUKI, T., IKUSHIMA, A. & MARUKAWA, K. (1963). *J. Phys. Soc., Japan*, **18** (Supplement II), 111.
LADELL, J., PARRISH, W. & TAYLOR, J. (1959). *Acta Cryst.* **12**, 253.
NAKAJIMA, K. & NUMAKURA, K. (1965). *Phil. Mag.* **12**, 361.
PAPOULIS, A. (1955). *Rev. Sci. Instrum.* **26**, 423.
RACHINGER, W. A. (1948). *J. Sci. Instrum.* **25**, 254.
SEEGER, A. (1955). *Defects in Crystalline Solids*. Report of Bristol Conference, p. 328. London: Physical Society.
SEEGER, A. (1957). *Dislocations and Mechanical Properties of Crystals*, p. 243. New York: John Wiley.
SEN GUPTA, S. P. & QUADER, M. A. (1966). *Acta Cryst.* **20**, 798.
STOKES, A. R. (1948). *Proc. Phys. Soc. London*, **B61**, 382.
SUZUKI, H. (1962). *J. Phys. Soc., Japan*, **17**, 522.
VASSAMILLET, L. F. & MASSALSKI, T. B. (1964). *J. Appl. Phys.* **35**, 2629.
WAGNER, C. N. J. (1957). *Acta Metallurg.* **5**, 427.
WARREN, B. E. & WAREKOIS, E. P. (1955). *Acta Metallurg.* **3**, 473.
WARREN, B. E. (1959). *Progr. Metal Phys.* **8**, 147.
WARREN, B. E. (1961). *J. Appl. Phys.* **32**, 2428.
WILLIS, B. T. M. (1959). *Acta Cryst.* **12**, 683.

Acta Cryst. (1967). **22**, 85

The Crystal Structure of Protactinium Pentachloride

BY RICHARD P. DODGE,* GORDON S. SMITH, QUINTIN JOHNSON AND ROBERT E. ELSON
University of California, Lawrence Radiation Laboratory, Livermore, California, U.S.A.

(*Received* 22 *March* 1966 *and in revised form* 5 *July* 1966)

$PaCl_5$ forms monoclinic crystals with lattice constants $a=7{\cdot}97$, $b=11{\cdot}35$, $c=8{\cdot}36$ Å; $\beta=106{\cdot}4°$. The probable space group is $C2/c$, and the unit cell contains four $PaCl_5$ units. The structure consists of infinite chains of non-regular pentagonal bipyramidal $PaCl_7$ groups which share pentagon edges. $PaCl_5$ therefore provides an example of the comparatively rare coordination number of seven, and illustrates a new way of achieving an overall stoichiometry of 1:5. Pa-Cl bond distances fall into two classes: (*a*) 2·43 (twice) and 2·46 Å to non-bridging Cl, and (*b*) 2·70 (twice) and 2·76 Å (twice) to bridging Cl. The Cl–Pa–Cl bond angle along the axis of the pentagon is $176\pm1°$.

Introduction

Chlorine compounds of protactinium (element 91) were first prepared by Grosse (1934), who reported a transparent, nearly colorless pentachloride melting at 301 °C and sublimable below its melting point. Only microgram amounts being available, no chemical analysis was carried out, and the formulation as a pentachloride was predicated by an expected analogy with the pentachlorides of Nb^V and Ta^V. The present crystal-structure analysis was undertaken to confirm the stoichiometry as well as to provide structural data on the volatile chloride. Of especial interest was whether the molecular structure would prove to be similar to that found for the pentachlorides of niobium and tantalum (Zalkin & Sands, 1958).

* Permanent address: Chemistry Department, University of the Pacific, Stockton, California, U.S.A.

Experimental

Our sample of protactinium, in the form of $PaO_{2\cdot25}$ was received from Oak Ridge National Laboratory. This sample, originally part of a gram-scale lot recovered by investigators at the Atomic Energy Research Establishment, Harwell, England, is now known to contain about 4% Nb [for further details see Stein (1964)]. The pentachloride was prepared as previously reported (Elson, 1954), namely, by the action of carbon tetrachloride on the oxide at about 200 °C, followed by a fractional sublimation to separate out a less volatile component (possibly $PaOCl_3$). These compounds are highly sensitive to atmospheric moisture and are radioactive as well (the most stable isotope, ^{231}Pa, is an α emitter). Manipulations during the preparative stages were performed in a (glass) vacuum system. Samples for X-ray diffraction photography were then sealed off in thin-walled glass capillaries.